

Changes in the Geometrical Shape of a Liquid Metal Pool in Relation to a Heat Input during a Welding Process

Abstract: The article aims to present a number of factors affecting the geometrical shape of a liquid metal pool when making welded joints, i.e. factors increasing or decreasing a heat input including the density and efficiency of welding power sources, stirring efficiency, tungsten electrode tip point, heat flow in a material being welded, cooling rate and linear energy supplied to a joint.

Keywords: welding power source, welding linear energy, heat flow, liquid metal pool

DOI: [10.17729/ebis.2017.3/7](https://doi.org/10.17729/ebis.2017.3/7)

Introduction

The computer-aided simulation of welding processes facilitates the proper and optimum development of a welding technology enabling the obtainment of required joint properties. The modelling of welding processes makes it possible to forecast and eliminate or minimise welding stresses and strains or the formation of unfavourable structures. Simulations enable the verification of the welding process course in various conditions, which is often impossible in industry due to high costs and laboriousness.

As physical phenomena taking place during welding are complex, their attempted modelling should allow for issues concerned with metal science, metallurgy, thermodynamics and mechanics. The modelling of welding processes requires both simplification and the extensive knowledge about the course of welding processes and their phenomena. The effect of heat on the material properties and the geometrical shape of the weld pool is non-linear, which additionally increases the complexity of the issue.

To increase the certainty of performed simulations it is necessary to perform a number of tests determining the influence of linear energy, heat input to the joint, welding rate and other factors affecting changes in the geometrical shape of the liquid metal pool and the structure of joints made using various welding processes.

Results of the above-named tests may be used as input data identifying the effect of welding parameters on structural changes in welds and changes in the geometrical shape of the liquid metal pool in programmes for the computer-aided support of welding processes, e.g. SYSWELD, SIMUFACT, WELDING or VIRFAC.

Changes in the Geometrical Shape of the Liquid Metal Pool

The geometrical shape of the liquid metal pool is influenced by a number of factors affecting the volume, width, length and depth of liquid metal. The article aims to present the effect of heat on the geometrical shape of the liquid metal pool.

An increase in heat source power density is accompanied by a decrease in a heat input to a material being welded. The slow heating of the welding area using a welding power source characterised by low power density leads to the discharge of a significant amount of heat from the welding area, before the liquid metal pool is formed, which, in turn, could trigger unfavourable structural changes. On the other hand, the same material exposed to the effect of a high-power welding power source melts instantly creating a joint with full penetration. High-power welding power sources enable a smaller heat input to a joint [1], allow the reduction of heat affected zones and make it possible to increase heat discharge rates. Figure 1 presents the correlation between a heat input to the joint and a welding power source applied in the process (power density).

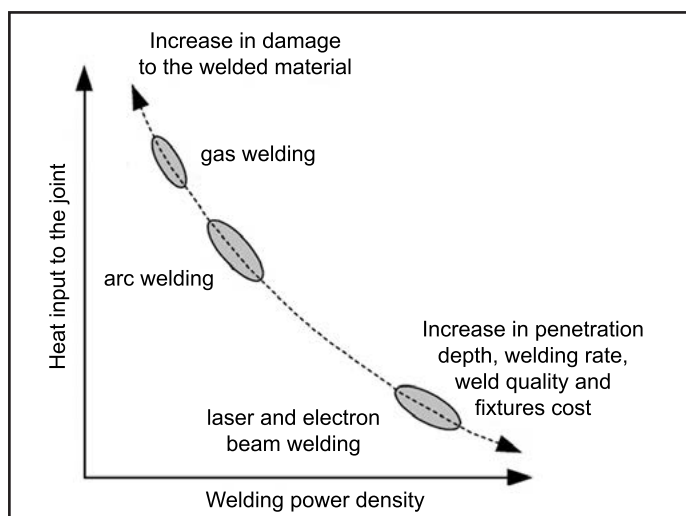


Fig. 1. Diagram presenting the dependence of a heat input to the joint on welding power density [1]

An increase in the power density of the welding power source should be accompanied by an increase in the liquid metal pool penetration depth as well as by a decrease in the liquid metal pool width and length. Another factor affecting the geometrical shape of the weld pool is the efficiency of welding power sources η defined by the following formula (1):

$$\eta = \frac{Qt_s}{Q_n t_s} = \frac{Q}{Q_n}$$

where:

- Q – heat input supplied to the welded material by welding power source, J,
- Q_n – nominal power of welding power source, J,
- t_s – welding time, s.

During welding processes, the welding power source provides energy enabling the melting of elements to be joined, yet it also escapes to the environment, thus leading to the reduction of efficiency and, consequently, to a decrease in $\eta < 1$. If efficiency is known, formula (1) can be used to determine heat input Q to the material being welded [1].

The efficiency of electric arc having constant voltage U and current I can be determined using the following formula (2):

$$\eta = \frac{Qt_s}{UIt_s} = \frac{Q}{Q_n}$$

where

- Q – heat input supplied to the welded material by welding power source, J,
- Q_n – nominal power of the welding power source, J,
- t_s – welding time, s,
- U – arc voltage, V,
- I – welding current, A.

Equation (2) can also be used to calculate the efficiency of electron beam welding and laser welding, where Q_n signifies the laser beam power (e.g. 2500 w). The heat input is defined as Q_n/v or UI/v , where v signifies the welding rate [1].

The welding power source efficiency in relation to various welding methods is presented in Figure 2. During laser welding, the efficiency of the welding power source is very low because of high beam reflexivity against the material being welded. This issue can be prevented by the fogging or oxidation of the surface. In turn, the efficiency of plasma welding is significantly higher than that of laser welding because of the significantly lower reflexivity of contracted arc energy beam [1].

The TIG method ($\eta=0.45\div0.60$ according to [2]), by contrast with plasma welding, does

not entail slight energy losses occurring when plasma arc is in contact with the water-cooled welding torch tip. During DC welding with the reversed polarity (-) electrode, electrons constitute the primary source of energy, releasing it in the form of heat when striking the material surface (high process efficiency). During DC welding with the straight polarity (+) electrode, electrons bombard primarily the electrode, slightly heating the area being welded in comparison with reversed polarity (considerable decrease in process efficiency). In turn, during AC welding, electrons transfer energy only during a half of a reversed polarity cycle [1].

In the MAG method ($\eta=0.45\div0.65$ according to [2]) and EO ($\eta=0.70\div0.85$ according to [2]), by contrast with the TIG method, energy is also transferred by heated filler metal (electrode) drops, increasing process efficiency [1].

During submerged arc welding ($\eta=0.80\div0.95$ according to [2]) electric arc burns under the layer of slag thermally isolating weld metal, decreasing heat losses caused by the contact with the environment, and increasing process efficiency [1].

The highest thermal efficiency is characteristic of electron beam welding with full penetration. The efficiency of such a welding power source is very high [1].

The stirring of material in the weld is referred to as stirring efficiency. Figure 3 presents cross-sections of representative areas revealing the contents of both base material and filler metal in the weld.

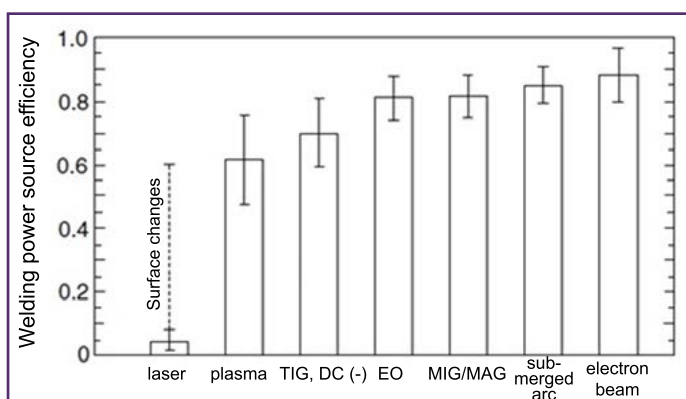


Fig. 2. Comparison of efficiencies of various welding power sources [1]

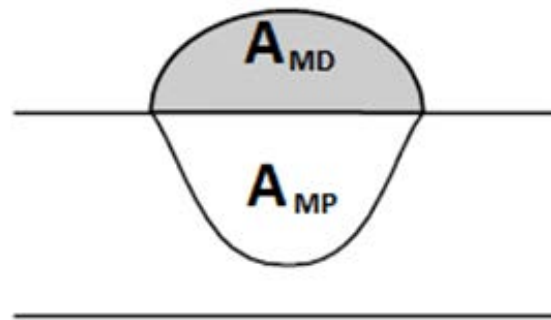


Fig. 3. Cross-section of the weld presenting areas filled with the filler metal (A_{MD}) and base material (A_{MP}) [1]

Stirring efficiency η_w can be identified based on the following formula [1]:

$$\eta_w = \frac{(A_{MP}Vt_s)H_{MP} + (A_{MD}Vt_s)H_{MD}}{\eta EI t_s}$$

where

- v – welding rate, mm/s,
- H_{MP} – energy necessary to heat the base material up to the melting point and its subsequent melting, J/mm³,
- H_{MD} – energy necessary to heat the filler metal up to the melting point and its subsequent melting, J/mm³,
- A_{MD} – weld areas filled with the filler metal, mm²,
- A_{MP} – weld areas filled with the base material, mm²,
- η – welding power source efficiency,
- U – welding arc voltage, V,
- EI – heat input, W,
- t_s – welding time, s.

The above-presented formula justifies the conclusion that the efficiency of stirring increases along with a decreasing welding rate. Stirring efficiency also grows if energy necessary for the heating of the filler metal and base material is lower. In turn, lower stirring efficiency should correspond to decreasing welding power source efficiency, increasing welding voltage and current and longer welding times. Stirring efficiency is also affected by the discharge of heat from the welding area. For instance, as heat discharge in copper alloys is significantly higher than in steels, a heat input to the joint should be much greater so that the joint could be made.

Figure 4 presents the cross-section of the weld revealing stirring-related differences corresponding to the use of various welding parameters [3].

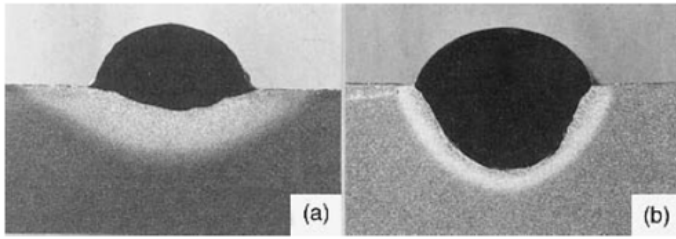


Fig. 4. Cross-section of the weld made on steel sheets with various stirring efficiency; weld a) was made using $V = 10$ mm/s and $UI = 1825$ W; weld b) $V = 26$ mm/s and $UI = 10170$ W [3]

During TIG welding, the angle of non-consumable electrode tip pointing significantly affected the geometrical shape and the operating manner of the electric arc and its power density. The increase in the electrode tip pointing angle was accompanied by the decrease in the electric arc diameter and the increase in power density (see Fig. 5) [1].

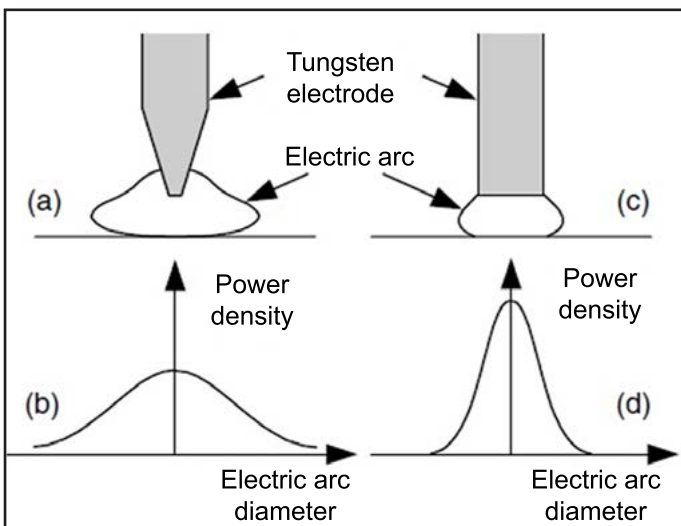


Fig. 5. Effect of electrode tip pointing angle on the shape of and power density of electric arc in TIG welding [1]

Further illustrations were created based on tests performed using the same current parameters, welding rate and the same distance between the electrode and the material being melted [4, 5]. Figure 6 presents the contraction of electric arc along with the increase in the electrode cone angle during TIG welding [4].

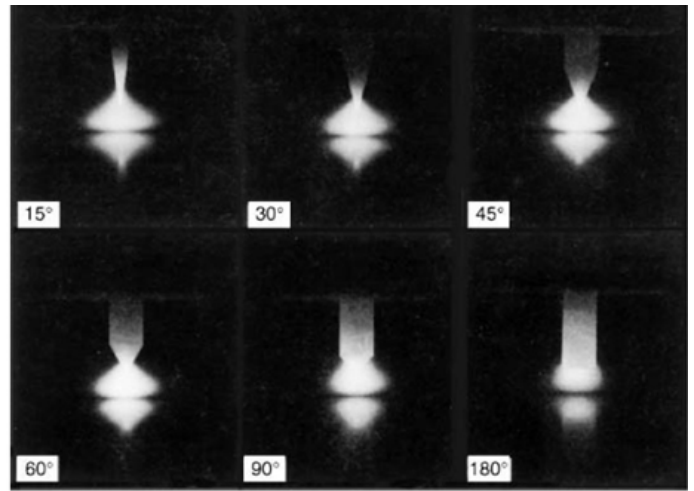


Fig. 6. Effect of electrode tip pointing angle on the shape of electric arc in TIG welding [4]

Changes in the width of electric arc also affected the penetration depth and the width of the run (Fig. 7). The greater the electrode pointing angle, the deeper the depth of penetration in the base material and the narrower the width.

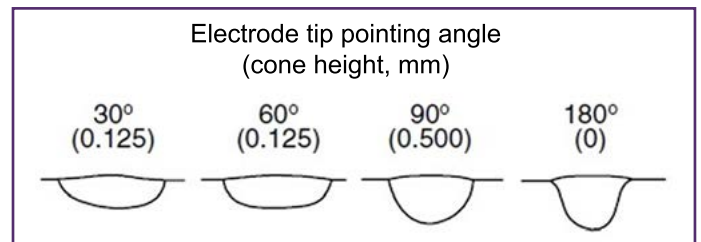


Fig. 7. Effect of non-consumable tungsten electrode pointing angle on the height and width of the penetration of TIG electric arc in the base material during the argon-shielded welding of stainless steel [5]

The geometrical dimensions of obtained welds/penetrations were also affected by the density of welding power source density (Fig. 8). In relation to the same heat input and welding rate, the depth of penetration decreased along with decreasing power density [6].

As can be seen in the above-presented examples, the appropriate adjustment of a tungsten electrode pointing angle enables the obtainment of the deeper and narrower geometrical shape of the liquid metal pool as well as the narrower heat affected zone. When simulating the flow of heat during the welding process the following can be assumed [7]:

- constant heat flow,
- spot welding power source,
- omission of crystallisation heat,

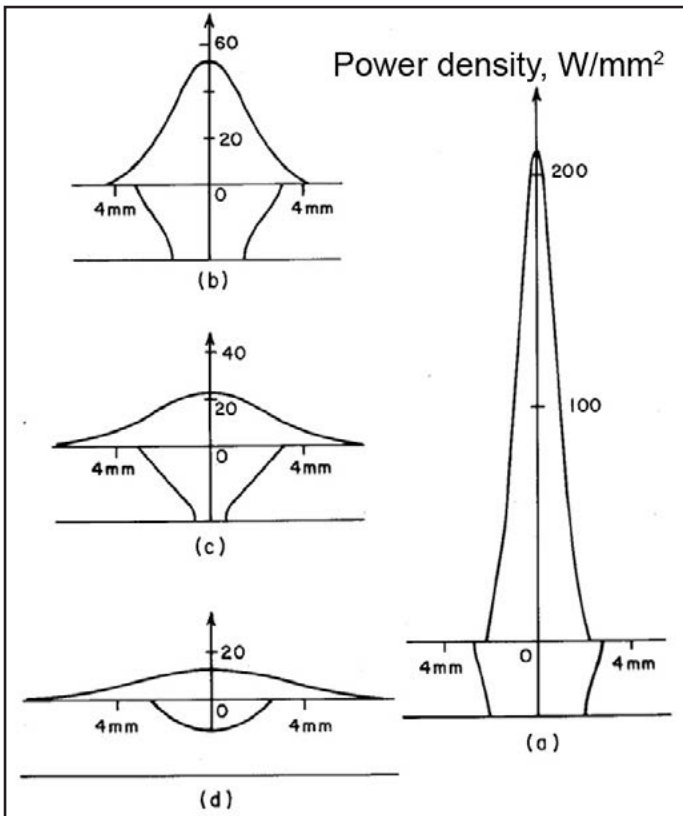


Fig. 8. Effect of heat source power density on the shape of the weld during the GTA welding of 3.2 mm thick aluminium sheet (6061) using a power of 880 W and a welding rate of 4.23 mm/s [6]

- constant heat properties,
- lack of heat losses from the surface of the material being welded,
- lack of convection in the liquid metal pool.

A linear energy input to a joint affects its post-weld cooling rate. The more energy is supplied to a joint, the more time is needed for a joint to cool down to ambient temperature (see Fig. 9). In turn, the scheme presented in Figure 10 presents temperature obtained by the welded joint and the heat affected zone in relation to a distance between the area of measurement and the central line of the joint.

The cooling rate increased along with the decrease in the thickness of the element subjected to welding. This could be attributed to the more favourable discharge of heat to the environment. The tests [9] revealed that, in relation to the same heat input and the same thickness of a sheet, the rate of cooling was shorter in terms of a T-joint than of a surfaced sheet. The above-presented phenomenon was caused by the faster discharge of heat to the environment [3, 10].

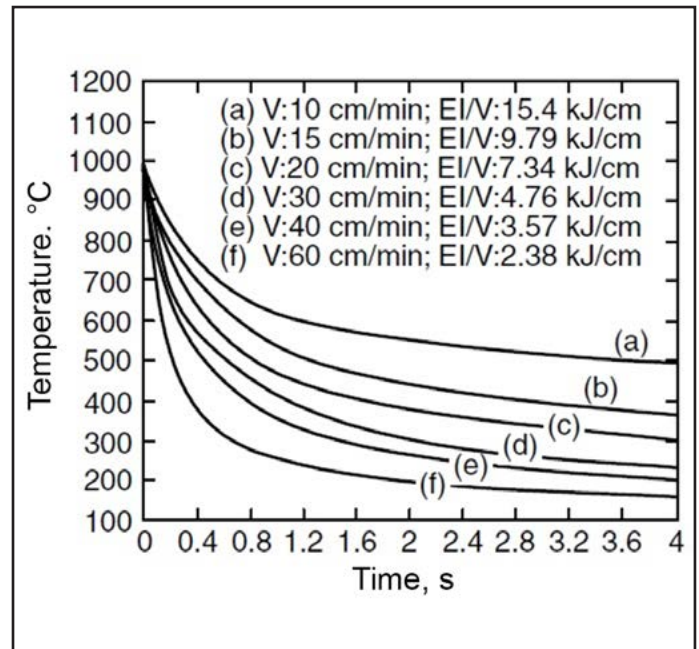


Fig. 9. Scheme presenting a cooling rate of a welded joint in relation to a heat input per a length unit [8]

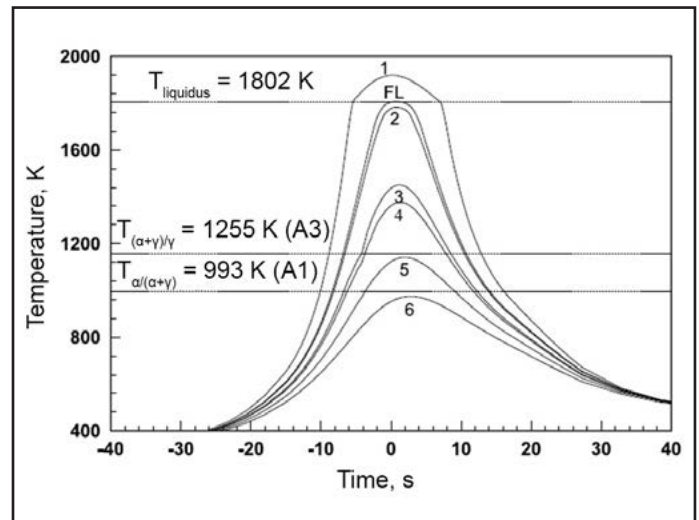


Fig. 10. Thermal cycles at various distances from the central line of the weld:
 1 – 2.5 mm, 2 – 4.5 mm, 3 – 5.5 mm, 4 – 5.75 mm, 5 – 6.75, 6 – 7.8 mm, FL: fusion line – 4.4 mm; above scheme was developed on the basis of GTA welding performed on steel AISI 1005 using a power of 1.9 kW [9]

The increase in linear energy was accompanied by the decrease in the cooling rate; the same applied to the heating of the joint before welding. Figure 11 presents the comparison of the welding rate in relation to joints made using the electroslag welding method (very high linear energy) and electric arc. The provided example illustrates the effect of a welding rate and preheating temperature on the post-weld cooling rate [11].

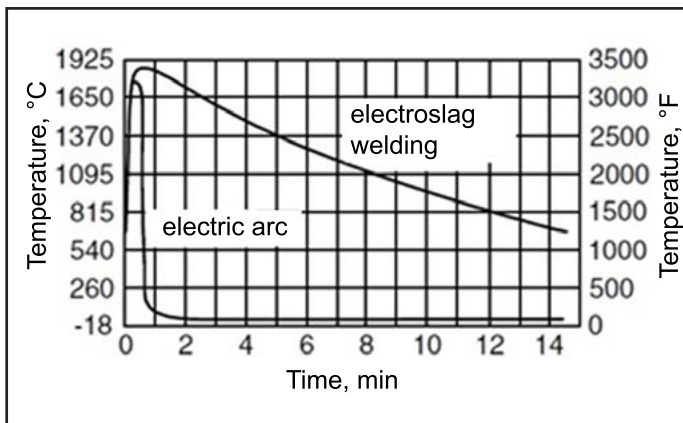


Fig. 11. Thermal cycles during arc welding and electroslag welding [11]

Summary

This article presents thermal factors which during welding may affect the geometrical shape of the weld pool. Further articles will present the effect of factors on changes in the geometrical shape of the liquid metal pool on the basis of results of tests performed in relation to various levels of linear energy and various welding processes. The research-related tests aim to obtain information so that computer-aided simulations of welding processes could represent their actual state as closely as possible. Examples of well performed computer simulations of welding processes were tests and numerical analyses performed in 2016 using steel X2CrNiMoN22-5-3 [12].

References

[1] Kou S.: *Welding Metallurgy*. Wiley-Interscience, New Jersey, 2003
<http://dx.doi.org/10.1002/0471434027>

[2] Tasak E.: *Metalurgia spawania*. JAK, Kraków, 2008.

[3] Kihara, H., Suzuki, H., Tamura, H.: *Researches on Weldable High-Strength Steels*. Society of Naval Architects of Japan, Tokyo, 1957

[4] Glickstein S. S.: *Temperature Measurements in Free Burning Arc*. *Welding Journal*, 1976, no. 8, pp. 222-229.

[5] Key J. F.: *Anode/Cathode Geometry and Shielding Gas Interrelationships in GTAW*. *Welding Journal*, 1980, no. 12, pp. 365-370.

[6] Kou S., Le Y.: *Three-dimensional Heat Flow and Solidification During and Autogenous GTA Welding of Aluminum Plates*. *Metallurgical and Materials Transaction A Journal*, 1983, no. 14A, pp. 2245-2253
<http://dx.doi.org/10.1007/bf02663298>

[7] Rosenthal D.: *Mathematical theory of heat distribution during welding and cutting*. *Welding Journal*, 1941, no. 5, pp. 220.

[8] Ward-Close C. M. (ed.): *Synthesis/Processing of Lightweight Metallic Materials II*. The Minerals, Metals and Materials Society, 1994, Warrendale, USA
<http://dx.doi.org/10.1002/chin.199824233>

[9] Zhang W., Elmer J.W., DebRoy T.: *Modeling and real time mapping of phases during GTA welding of 1005 steel*. *Materials Science and Engineering*, 2002, t. 333, no. 1-2, pp. 320-335
[http://dx.doi.org/10.1016/S0921-5093\(01\)01857-3](http://dx.doi.org/10.1016/S0921-5093(01)01857-3)

[10] Inagaki M., Sekiguchi H.: *Continuous cooling transformation diagrams for welding of Mn-Si type 2H steels*. *Transection of the National Research Institute Metals*, 1960, no. 2, pp. 102
http://dx.doi.org/10.2355/tetsutohagane1955.46.6_657

[11] Liu S., Brandi S. D., Thomas R. D.: *ASM Handbook*, vol. 6, ASM International.

[12] Giętka T., Ciechacki K., Kik T.: *Numerical Simulation of Duplex Steel Multipass Welding*. *Archives of Metallurgy and Materials*, 2016, t. 61, no. 4 pp. 1975-1984.
<http://dx.doi.org/10.1515/amm-2016-0319>